Jackknife stability of a tractor semi-trailer combination

TU/e Mechanical Engineering
Masterproject
2006-2007

Jackknife stability of a tractor semi-trailer combination

Author: **J.W.L.H. Maas (0529865)**

Tutor: **Prof. dr. H. Nijmeijer**

Eindhoven, 11 June 2007

Abstract

This report focusses on different aspects of jackknife instability of articulated trucks. Jackknife instability is a form of lateral instability where the tractor pivots backward into the trailer. By doing simulations of a simplified bicycle model and evaluating the eigenvalues of the system, it is investigated what exactly causes jackknife instability. It is found that adjusting the system parameters can cause the system to become unstable when the parameters are not selected properly. Also, system inputs such as brake force can cause the system to become unstable. Finally, two different systems are analyzed which can help prevent jackknife instability. These systems are Active Yaw Control (AYC) and Active Front Steering (AFS). An AYC system uses variable braking forces on separate tires, whereas an AFS system uses a variable steering gear ratio.

Table of contents

List of symbols

Symbol	Unit	Description
α	rad	Tire side slip angle
a	m	Distance from front tire of the tractor to the centre of gravity of the tractor
β	rad	Vehicle side slip angle
b	m	Distance from the centre of gravity of the tractor to the rear tires of the tractor
B	N.m.s/rad	Damping
c	m	Distance from the centre of gravity of the tractor to the pivot point of the vehicle
C_α	N/rad	Tire cornering stiffness
δ	rad	Steering angle
d	m	Distance from the pivot point of the vehicle to the centre of gravity of the trailer
e	m	Distance from the centre of gravity of the trailer to the rear wheels of the trailer
F	N	Force
γ	rad	Articulation angle
J	$kg.m^2$	Inertia
K	N.m/rad	Self-aligning stiffness
λ	-	Eigenvalue
m	kg	Mass
r	rad/s	Yaw rate
P	Pa	Braking pressure
q	rad/s	Articulation rate
τ	N.m	Torque
μ	-	Road friction coefficient
u	m/s	Longitudinal velocity
v	m/s	Lateral velocity
ω_n	rad/s	Natural frequency
ω_o	rad/s	Natural frequency of the undamped system
ψ	rad	Vehicle yaw angle
ζ	-	Damping ratio

Indexes	Unit	Description
$(..)_1$	-	Front tire of the tractor (in case of force, cornering stiffness and side slip angle)
$(..)_1$	-	Tractor (in case of mass and inertia)
$(..)_2$	-	Rear tire of the tractor (in case of force, cornering stiffness and side slip angle)
$(..)_2$	-	Trailer (in case of mass and inertia)
$(..)_3$	-	Tire of the trailer (in case of force and cornering stiffness and side slip angle)
$(..)_{ABS}$	-	Anti-lock braking system
$(..)_{afs}$	-	Active front steering
$(..)_{AYC}$	-	Active yaw control
$(..)_d$	-	Desired
$(..)_{drv}$	-	Driver
$(..)_{hw}$	-	Handwheel
$(..)_{max}$	-	Maximum value
$(..)_s$	-	Steering system
$(..)_x$	-	Longitudinal direction
$(..)_z$	-	Vertical direction

1. Introduction

As a result of the increasing demand on load capacities of trucks, problems may occur when it comes to stability of trucks. The most important stability problems occur when lateral acceleration becomes too high (roll-over) or when the tractor pivots backward into the trailer (jackknife). A jackknife can occur for example due to slippery roads, hard braking or shifting loads. This form of instability is discussed in this report. Over the years, many systems to reduce jackknife instability are developed. Two systems that are discussed in this report are Active Yaw Control (AYC) and Active Front Steering (AFS).

To get insight in what causes large truck crashes, studies are performed by several organizations. One of these studies is the Large-Truck Crash Causation Study [1]. It is conducted in the United States and the crashes that are examined occurred from April 1, 2001, through December 31, 2003. The study shows that of all examined multivehicle crashes regarding trucks causing the accident, 9% is due to a jackknife event. Another report is published by the National Highway Traffic Safety Administration. This report [2] is based on traffic accidents in the United States in 2003. It shows that 3.1% of all examined crashes caused by tractor-trailer combinations is due to a jackknife event. Moreover, 7.1% of all examined fatal crashes caused by tractor-trailer combinations is due to a jackknife event.

The problem that is discussed in this report is what exactly causes jackknifing and what can be done to prevent this instability. This is done by running simulations in Matlab and a literature study respectively. The simulations in Matlab are done by using a simplified model of a tractor semi-trailer combination.

The remainder of this report is organized as follows:
First, the modeling of the tractor semi-trailer combination is discussed in chapter 2. In chapter 3, a way to determine the worst-case brake- and steering input is given. After that, simulations with a linear bicycle model are made in chapter 4. A stability analysis is made for various vehicle parameters (chapter 5) and for varying cornering stiffnesses during braking (chapter 6). In chapters 7 and 8, two systems that can reduce or prevent jackknife instability are discussed. The final chapter contains the conclusions and recommendations.

2. Modeling

The first step towards simulation is building a model for the tractor-semitrailer. The model that is discussed is a simple bicycle model. Before building the model, some symbols have to be assigned to the variables and states. These are depicted in figure 2.1.

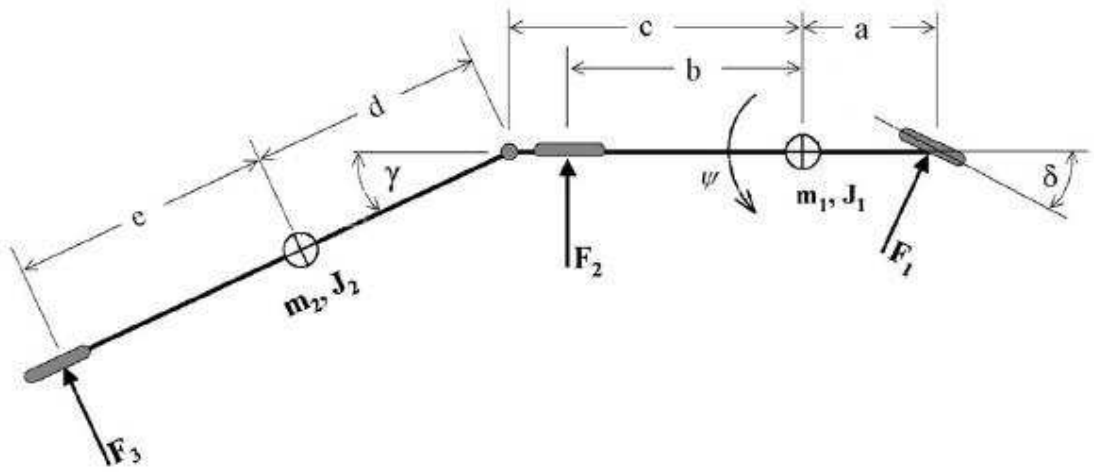

Figure 2.1 Schematic representation of the 3-axle bicycle model

2.1 Equations of motion

The equations of motions for this system are given as

$$\left(m_1+m_2\right)\left(\dot{v}+ur\right)-m_2\left(c+d\right)\ddot{\psi}-m_2d\ddot{\gamma}=F_1+F_2+F_3 \tag{2.1}$$

$$\begin{aligned}&-m_2\left(c+d\right)\left[\dot{v}+ur\right]+\left[J_1+J_2+m_2\left(c+d\right)^2\right]\dot{r}+\left(J_2+m_2d^2\right)\dot{q}=\ldots\\&=aF_1-bF_2-F_3\left(c+d+e\right)\end{aligned} \tag{2.2}$$

$$-m_2d\left(\dot{v}+ur\right)+\left[J_2+m_2d\left(c+d\right)\right]\dot{r}+\left(J_2+m_2d^2\right)\dot{q}=-F_3\left(d+e\right) \tag{2.3}$$

with:

$m_1 =$ mass of the tractor

$m_2 =$ mass of the trailer

$v =$ vehicle lateral velocity

$u =$ vehicle longitudinal velocity

$r =$ vehicle yaw rate

$a, b, c, d, e =$ vehicle characteristic lengths (figure 2.1)

$\psi =$ vehicle yaw angle

$\gamma =$ articulation angle

$F_1, F_2, F_3 =$ tyre cornering forces

$J_1 =$ tractor moment of inertia

$J_2 =$ trailer moment of inertia

$q =$ articulation rate

These equations of motion agree with Pacejka's equations in [3]. The tire cornering forces can be described as

$$F_i = -C_i \alpha_i \qquad \text{for } i = 1, 2, 3 \tag{2.4}$$

with:

$C =$ tire cornering stiffness

$\alpha =$ tire side slip angle

The linearized equations for α are given as

$$\alpha_1 = \frac{v + ar}{u} - \delta \tag{2.5}$$

$$\alpha_2 = \frac{v - br}{u} \tag{2.6}$$

$$\alpha_3 = \frac{v - (c + d + e) r - (d + e) q}{u} - \gamma \tag{2.7}$$

with:

$\delta =$ steering angle

A combination of (2.1) through (2.7) can be transformed into a first-order system in matrix form. This matrix form can be described as

$$M\dot{x} = Kx + B_1 u \tag{2.8}$$

with:

M = mass matrix

K = stiffness matrix

B_1 = input matrix

For the representation in (2.8), the state vector and the derivative of the state vector are given as

$$x = \begin{bmatrix} \dot{y} \\ \dot{\psi} \\ \dot{\gamma} \\ \gamma \end{bmatrix} = \begin{bmatrix} v \\ r \\ q \\ \gamma \end{bmatrix} = \begin{bmatrix} \text{vehicle lateral velocity} \\ \text{vehicle yaw rate} \\ \text{articulation rate} \\ \text{articulation angle} \end{bmatrix} \tag{2.9}$$

$$\dot{x} = \begin{bmatrix} \ddot{y} \\ \ddot{\psi} \\ \ddot{\gamma} \\ \dot{\gamma} \end{bmatrix} = \begin{bmatrix} \dot{v} \\ \dot{r} \\ \dot{q} \\ \dot{\gamma} \end{bmatrix} = \begin{bmatrix} \text{vehicle lateral acceleration} \\ \text{vehicle yaw acceleration} \\ \text{articulation acceleration} \\ \text{articulation rate} \end{bmatrix} \tag{2.10}$$

The matrices M, K and B_1 are given in appendix A.

2.2 State-space form

In order to observe the dynamics of the model, the model is manipulated to be represented in state-space format, shown as

$$\dot{x} = Ax + Bu \tag{2.11}$$

When the forward velocity and cornering stiffnesses are assumed to be constant, the matrix A is time-independent. The formulation in (2.8) is converted into state-space format using the transformation with

$$A = M^{-1}K \tag{2.12}$$

$$B = M^{-1}B_1 \tag{2.13}$$

3. Worst-case maneuvers

The problem that is discussed in this chapter is what combination of brake and steering inputs is the most dangerous for the truck, in the sense of jackknife when both inputs are limited below a certain threshold value. Moreover, when can we guarantee that no jackknife could occur under certain initial speed and road friction conditions?

3.1 Worst-case problems formulation

Worst-case evaluation problems can be divided into four types [4]: one player without preview information (lP), one player with preview information (lPP), two players without preview information (2P), and two players with preview information (2PP). The two-player types are applicable to systems with both control and disturbance inputs and when their objectives are opposite. The preview cases should be applied when one of the players could "peek into the future" against its opponent. The preview information, in fact, usually arises from the delays of system components. The jackknife of articulated trucks is formulated as a 1P problem, for which we want to identify the worst-case inputs (steering and braking).

The dynamics of the vehicle are assumed to be in state-space form, described as

$$\begin{aligned} \dot{\underline{x}}(t) &= f(\underline{x}(t), \underline{w}(t), t) \\ \underline{x}(0) &= \underline{x}_0 \end{aligned} \qquad (3.1)$$

with:
$\underline{x}(t) =$ state vector
$\underline{w}(t) =$ disturbance vector

The disturbance vector is assumed to be governed by the worst-case algorithm, which represents the worst possible action that could come from a human driver. It is assumed that the goal of $\underline{w}(t)$ is to maximize a cost function [5] described as

$$J(\underline{x}(t), \underline{w}(t), t) = \int_{t_0}^{t_f} \left\{ \underline{x}^T(t) Q \underline{x}(t) - \underline{w}^T(t) P \underline{w}(t) \right\} dt \qquad (3.2)$$

where Q and P are weighting matrices that are positive semi-definite and positive definite respectively. The matrices P and Q are selected in such a way that a large penalty is imposed on the variable that is most important for the selected stability evaluation. For example, in the jackknife case, this variable is the articulation angle. Theoretically, only the relative size between P and Q matters. Therefore, P could be selected to be an identity matrix. However, elements of P actually determine the convergence rate of the nonlinear learning algorithm. This 1P formulation defined by (3.1) and (3.2) is a standard optimization problem. By replacing the nonlinear dynamics with linear state matrix (2.11), the optimal solution to the optimization problem, (3.1) and (3.2), is known to be [6]

$$\underline{w}(t)^* = -P^{-1}D^T K(t)\underline{x}(t) \tag{3.3}$$

where K is the solution of the Riccati differential equation

$$\begin{aligned} \dot{K}(t) &= -A^T K(t) - K(t)A + K(t)DP^{-1}D^T K(t) + Q \\ K(t_f) &= 0 \end{aligned} \tag{3.4}$$

3.2 Sensitivity

In the past, the research focus has been on the relationship between this instability mode and vehicle parameters. Even though this relationship can easily be found with current simulation technologies, it is not clear how to generate “bad” steering and braking inputs leading to truck jackknifing. An option is to introduce a general “bad” maneuver to apply to a vehicle and determine the stability of the vehicle based on the response of this vehicle to this maneuver. This option is similar to Dugoff’s “drastic maneuver” [7]. A drastic maneuver may be proposed for jackknife events as well. However, the selected maneuver may favor one vehicle over others and may not be a fair basis for determining a tendency to jackknife. The worst-case vehicle evaluation methodology (section 3.1) identifies the weak link of each individual vehicle and generates the worst-case maneuvers accordingly. Therefore, the vehicle performance can be more fairly assessed.

3.3 Simulation

Arcsim is a program that describes 3D motions of a truck using 79 state variables. Since not all these states are relevant for describing the jackknifing, many of these variables can be neglected.

To illustrate a jackknife, simulations can be done by using Arcsim. In these simulations, the truck is assumed to start from an initial speed of 60 mi/hr. When the cost function (3.2) is then modified to penalize the articulation angle between the tractor and the trailer, the "worst-case" steering and braking produce a large articulation angle. However, when the road friction is low enough, it is possible to get a jackknife even when the steering angle is small. To generate the truck jackknife, it is necessary to apply heavy braking for an extended period of time. Steering plays only a secondary role, which serves to generate initial perturbations to the yaw motion of the vehicle. A large articulation angle is then generated from the inverted pendulum nature of the articulated vehicle. This is shown in figure 3.1.

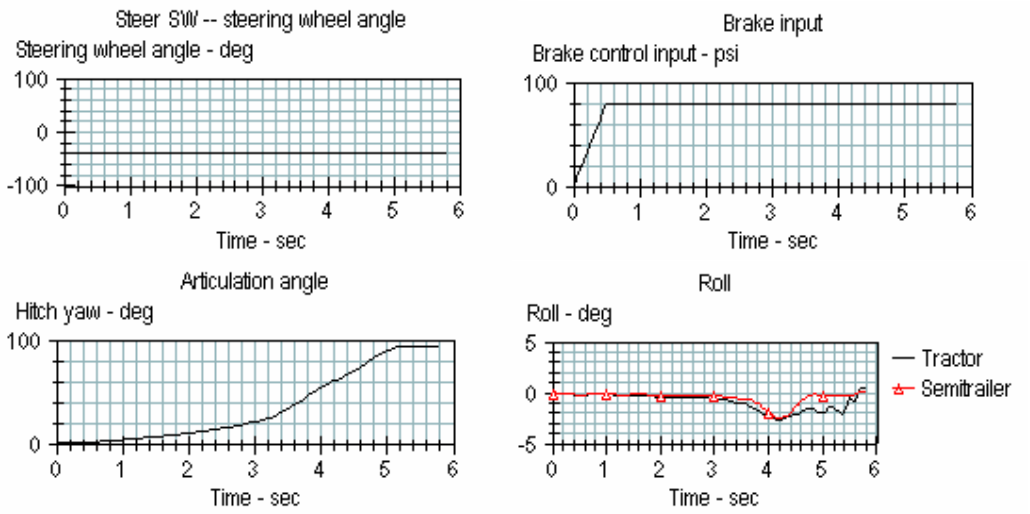

Figure 3.1 Vehicle response for inputs that cause a jackknife (μ =0.4)

One of the benefits of the worst-case evaluation method is to determine important vehicle and operational parameters involved in the truck jackknife.

3.4 Conclusions

In this chapter, it is shown that a worst-case evaluation determines the stability of each tractor-semitrailer combination separately. This is a better way to determine stability than a standardized "bad" maneuver, which may favor one vehicle over others. A worst-case evaluation determines the worst possible braking and steering input for each vehicle that could come from a driver.

4. Simulation of the linear model

Using the program Matlab, simulations can be made of the dynamics of the model. The matrices from the state-space form have been derived in section 2.2. With these matrices, linear simulations can be done with the *lsim* command in Matlab.

4.1 Parameters

Before a simulation can be made, the system parameters have to be determined. Table 4.1 shows some realistic values for the vehicle parameters and they are obtained from [8]. The parameters originally are determined for the TruckSim simulation program.

Table 4.1 Vehicle parameters

Parameter	Value	Unit
m_1	8812	kg
m_2	16484	kg
J_1	46100	$kg.m^2$
J_2	$4.5201.10^5$	$kg.m^2$
a	2.062	m
b	2.723	m
c	2.539	m
d	7.483	m
e	3.760	m
C_1	$3.8193.10^5$	N/rad
C_2	$7.3339.10^5$	N/rad
C_3	$8.8144.10^5$	N/rad

4.2 Linear simulation results

Using the *lsim* command in Matlab, simulations can be made with varying parameters and variables. In figure 4.1, the dynamic response is shown for a sinusoidal steering input with a frequency of 0.25 Hz and an amplitude of 0.1 rad. This is comparable to a lane change which consists of a sinusoidal steering input. The parameters are taken from table 4.1 and the longitudinal velocity is 20 m/s (=72 km/h), which is close to the legal speed limit in the Netherlands.

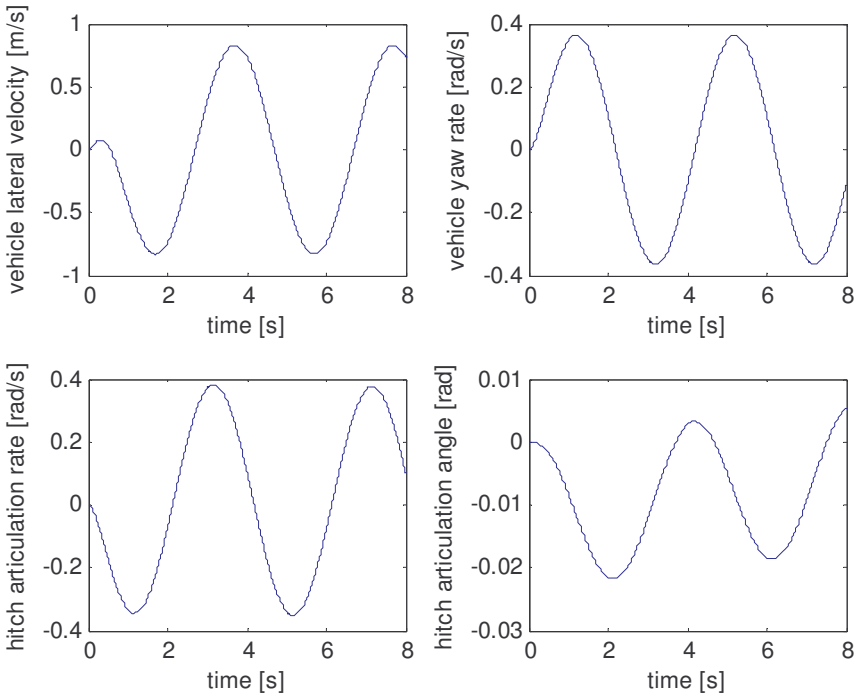

Figure 4.1 Vehicle response to a sinusoidal steering angle input

As can be seen from this figure, the system is stable. Simulations with other steering inputs can be made as well. In figure 4.2, the dynamic response of the system is shown for a step input for the steering angle of 1 rad after 1 second.

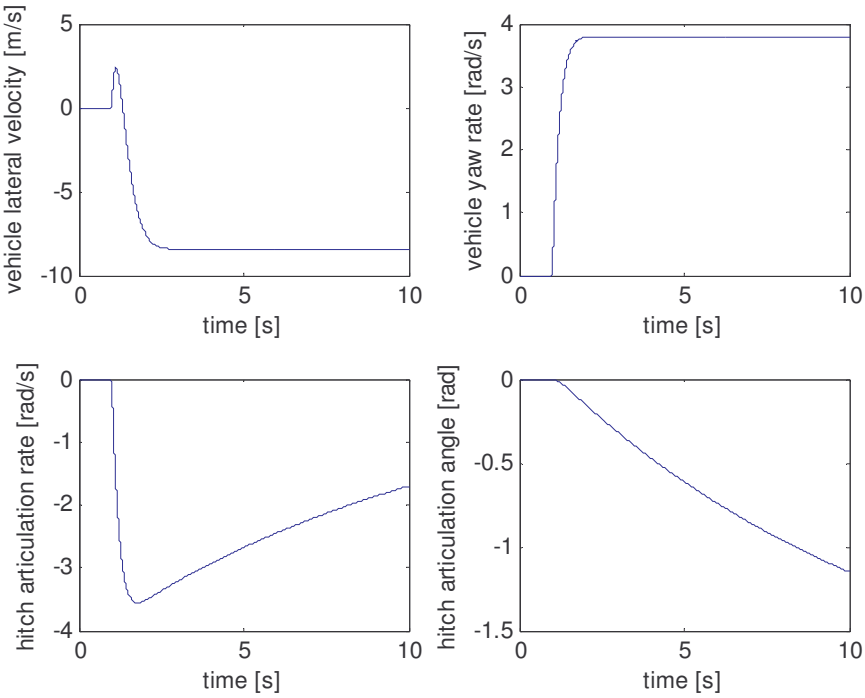

Figure 4.2 Dynamic response for a step steering input

As well as the input, the system parameters can be varied. Figure 4.3 shows the dynamic response to a step input for the steering angle for a cornering stiffness C_2 that is half the value with respect to the previous simulation. The rest of the parameters and variables are unchanged.

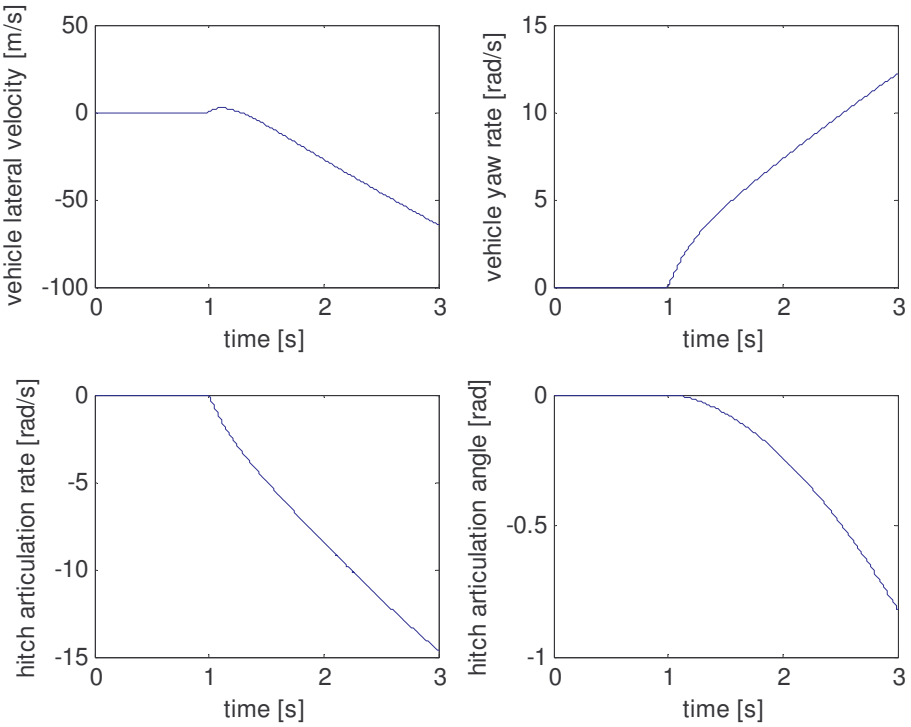

Figure 4.3 Dynamic response (blue) for a step steering input (grey) with reduced C_2

Clearly, it can be concluded from this simulation that the system becomes unstable. As a result of the linear simulation, at least one state goes to infinity when time goes to infinity. This is not possible in real situations, because an angle cannot become larger than 360 degrees. However, this gives an initial estimate of the stability of the system.

4.3 Conclusions

The stability of the system is dependent on the system parameters. From the simulations in this chapter it can be seen that a stable system can become unstable by varying only one parameter.

5. Stability

From section 4.2 it can be concluded that the stability of the system is dependent on the vehicle parameters. The stability of the system can be determined by computing the eigenvalues of the system matrix *A* from the state-space form (2.11).

5.1 Analysis on the baseline vehicle

With the system matrices of the state-space form from section 2.2, an analysis can be made regarding the stability of the system. Since the forward velocity and cornering stiffnesses are assumed to be constant, the system matrices are time-independent. The stability can then be analyzed by computing the eigenvalues of matrix *A*. Also, the natural frequency of the undamped system, the natural frequency and the damping ratio can be computed for this analysis as

$$\omega_o = \sqrt{\text{abs}(\text{Re}(\lambda)^2) + \text{abs}(\text{Im}(\lambda)^2)} \tag{5.1}$$

$$\omega_n = \text{abs}(\text{Im}(\lambda)) \tag{5.2}$$

$$\zeta = \frac{\text{abs}(\text{Re}(\lambda))}{\sqrt{\text{abs}(\text{Re}(\lambda)^2) + \text{abs}(\text{Im}(\lambda)^2)}} \tag{5.3}$$

with:

ω_o = natural frequency of the undamped system

ω_n = natural frequency

ζ = damping ratio

λ = eigenvalue

abs( ) = absolute value

Re( ) = real part

Im( ) = imaginary part

Table 5.1 shows the eigenvalues of a vehicle with parameters equal to those in table 4.1. A longitudinal velocity of 20 m/s (=72km/h) is taken for the analysis.

Table 5.1 Eigenvalues of the baseline vehicle at 20 m/s

Eigenvalue	Value	ω_o [rad/s]	ω_n [rad/s]	ζ [-]
λ_1	-0.0909	-	-	-
λ_2	-4.0683+1.3023i	4.2717	1.3023	0.9524
λ_3	-4.0683-1.3023i	4.2717	1.3023	0.9524
λ_4	-3.9993	-	-	-

From the table it can be seen that the real parts of all eigenvalues are negative, so the system is stable. The damping ratio's are close to 1, so the system is well damped. A

similar analysis can be performed with a velocity of 30 m/s (=108 km/h). The results are given in table 5.2.

Table 5.2 Eigenvalues of the baseline vehicle at 30 m/s

Eigenvalue	Value	ω_o	ω_n	ζ
λ_1	-2.7122+1.3170i	3.0150	1.3170	0.8996
λ_2	-2.7122-1.3170i	3.0150	1.3170	0.8996
λ_3	-0.0920	-	-	-
λ_4	-2.6347	-	-	-

The system is still stable, since the real parts of the eigenvalues are negative. However, the value of the natural frequency of the undamped system has decreased as well as the damping ratio.

5.2 Analysis on the system parameters

There are twelve system parameters that can be varied. For the stability analysis, the eigenvalues are again analyzed. First, the stability is analyzed when the cornering stiffness of the different tires is varied. This can be done as a function of the longitudinal velocity of the vehicle. This is shown in figure 5.1. The line separates the stable region from the unstable region. The parameters that are not varied are taken according to table 4.1 and are constant.

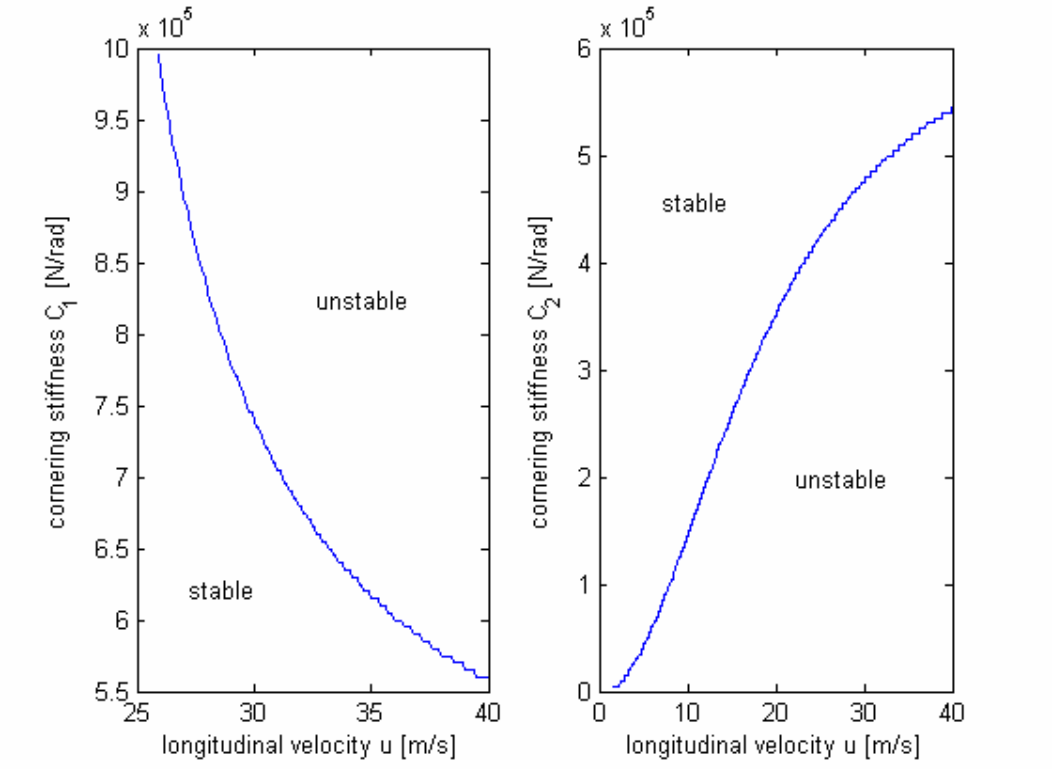

Figure 5.1 Stability for cornering stiffness versus longitudinal velocity

From figure 5.1, it can be concluded roughly that for increasing C_1 and u and for decreasing C_2 the system becomes unstable. However, it must be taken into account that the other parameters are kept constant at a certain value. The results are according to what can be expected in a real situation. An increasing C_1 and decreasing C_2 makes a vehicle more oversteered, while an increasing speed causes the damping ratio for the vehicle to decrease (section 5.1).

Simulations show that varying cornering stiffness C_3 cannot cause the system to become unstable regardless of longitudinal velocity, unless the cornering stiffness becomes negative. However, a negative cornering stiffness is not realistic. Although the system cannot become unstable, two of the eigenvalues have a real part that is exactly equal to 0 when the cornering stiffness C_3 is equal to 0.

Next, the mass of the tractor and trailer is analyzed. An assumption for this part is that the moment of inertia does not change. In practice, this can be regarded as removing mass near the centre of gravity. The results are shown in figure 5.2.

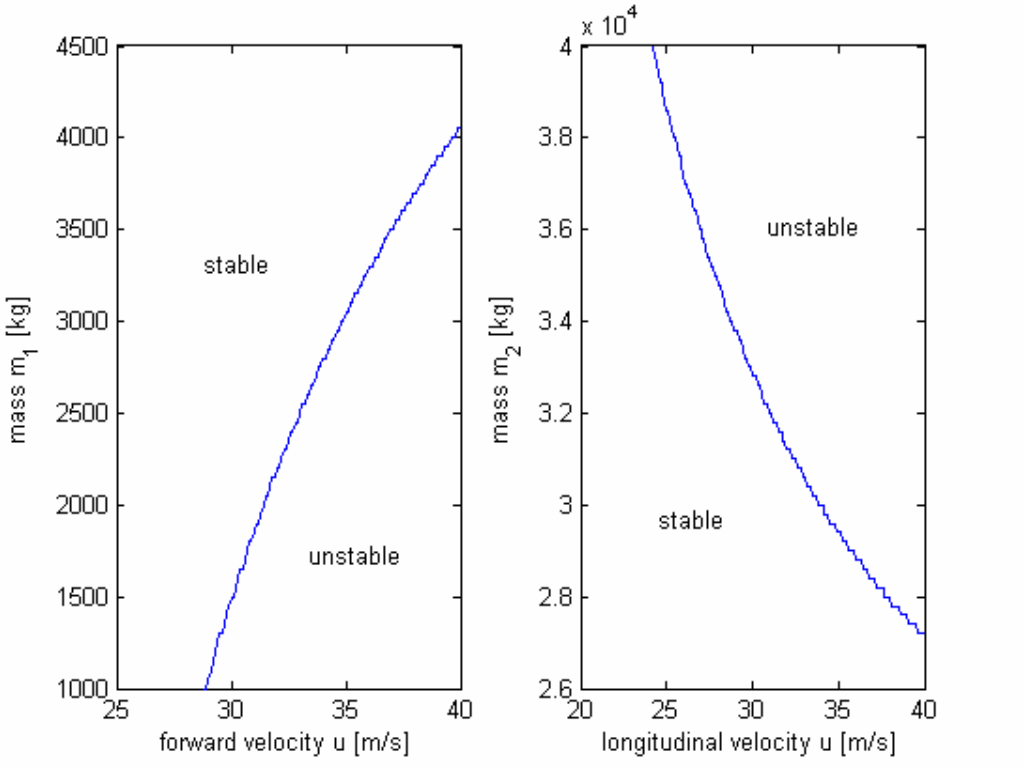

Figure 5.2 Stability for mass versus longitudinal velocity

From figure 5.2, it can be concluded that for decreasing m_1 and increasing m_2 the system becomes unstable. Again, it must be taken into account that the other parameters are kept constant at a certain value.

Simulations show that varying inertias J_1 and J_2 cannot cause the system to become unstable regardless of longitudinal velocity.

The last parameters that can be varied are the characteristic lengths of the vehicle shown in figure 2.1. The results are shown in figure 5.3 through 5.5.

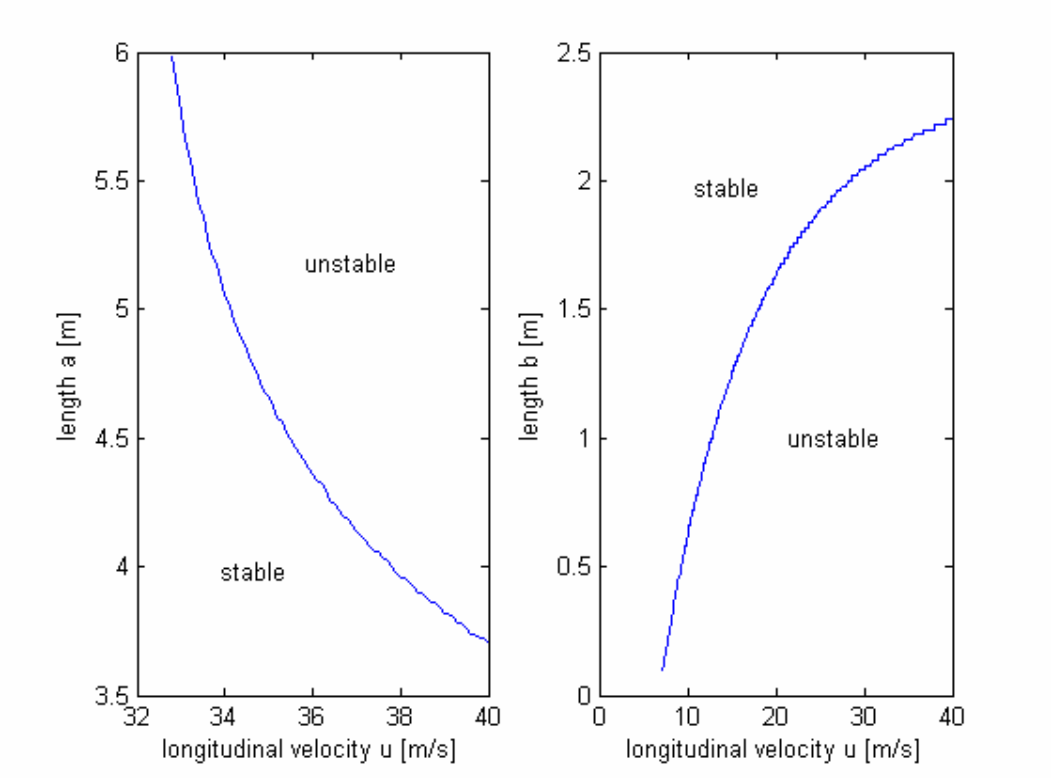

Figure 5.3 Stability for lengths *a* and *b* versus longitudinal velocity

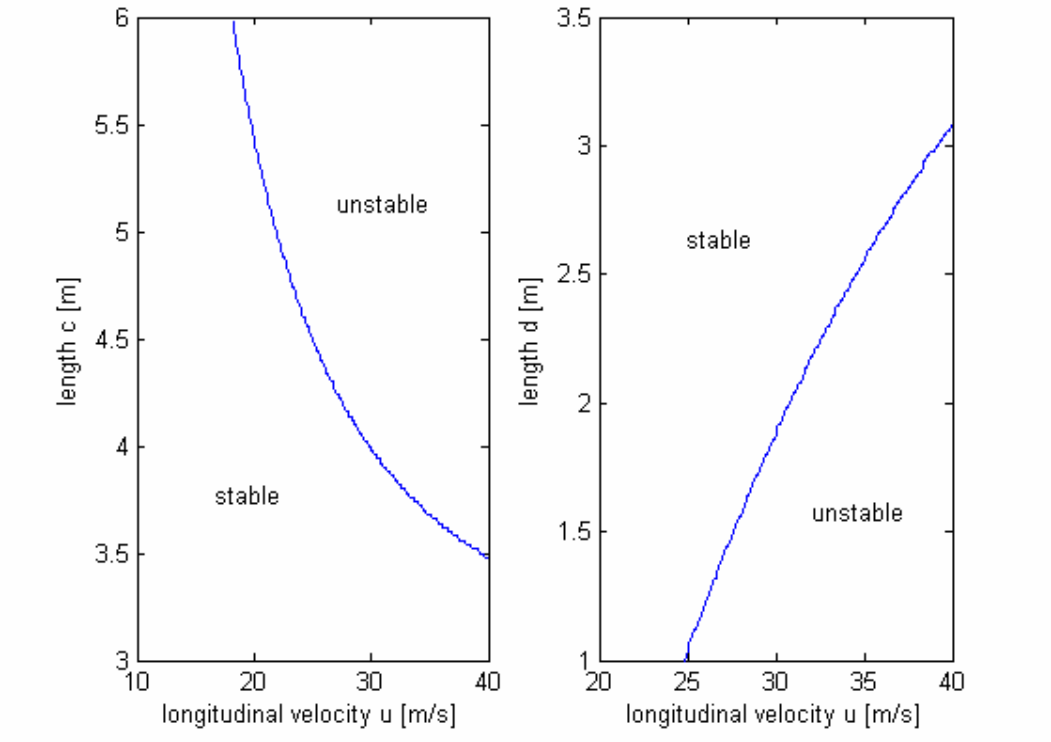

Figure 5.4 Stability for *b* versus *u*

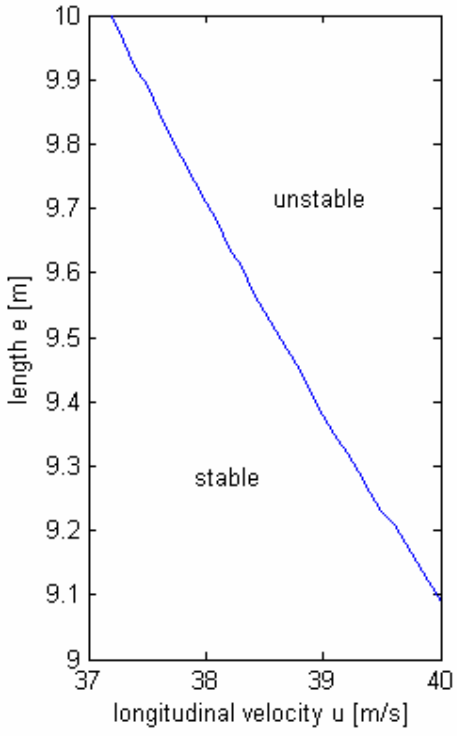

Figure 5.5 Stability for *e* versus *u*

From figure 5.3 through 5.5, it can be concluded that for decreasing b and d and increasing a, c, and e the system becomes unstable. Again, it must be taken into account that the other parameters are kept constant at a certain value.

When comparing the values from table 4.1 for the various system parameters to the stability results shown in figures 5.1 through 5.5, it can be seen that the parameters in table 4.1 are all in the stable region for realistic values of the longitudinal speed.

5.3 Conclusions

An increasing forward velocity can cause an articulated truck to become less stable. Besides the forward velocity, the system parameters can also cause the system to become less stable. The simulations in this chapter show that this is the case for increasing C_1, m_2, a, c and e and decreasing C_2, C_3, m_1, b and d.

6. Cornering stiffness during braking

As can be seen from chapter 5, parameters in the vehicle can be chosen so that the system is stable. However, unlike the other parameters, the cornering stiffness changes during different maneuvers. The cornering stiffness is dependent on the road friction coefficient, the vertical force and the longitudinal force on the tire. The focus in this chapter is on the dependency of the cornering stiffness on the longitudinal force (braking).

6.1 Dependency of cornering stiffness on longitudinal force

The dependency of the cornering stiffness on different variables is obtained from [3]:

$$C(\mu, F_z, F_x) = \varphi\left\{C(F_z) - \frac{1}{2}\mu F_z\right\} + \frac{1}{2}\left(\mu F_z - F_x\right) \tag{6.1}$$

with:

$$\varphi = \left\{1 - \left(\frac{Fx}{\mu Fz}\right)^n\right\}^{1/n} \tag{6.2}$$

Depending on the curvature, a value for n between 2 and 8 can be chosen. This is displayed in figure 6.1 where a possible cornering stiffness characteristic is given for different values of n.

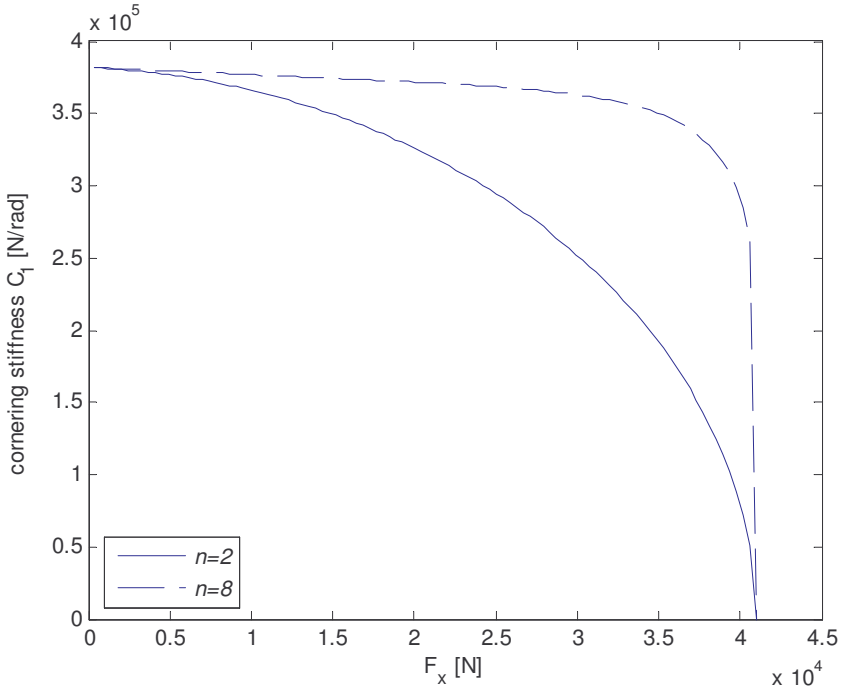

Figure 6.1 Cornering stiffness for different values of n

As can be seen from figure 6.1, the cornering stiffness drops to 0. This happens when $F_x = \mu F_z$ (wheel lock).

To apply a variable cornering stiffness to the model, the dependency of (6.1) and (6.2) have to be calculated for the vehicle with parameter values of table 4.1. The vertical forces can be calculated from:

$$F_{z1} = \left(\frac{b}{a+b}\right) m_1 g + \left(\frac{b-c}{a+b}\right)\left(\frac{e}{d+e}\right) m_2 g \tag{6.3}$$

$$F_{z2} = \left(\frac{a}{a+b}\right) m_1 g + \left(\frac{a+c}{a+b}\right)\left(\frac{e}{d+e}\right) m_2 g \tag{6.4}$$

$$F_{z3} = \left(\frac{d}{d+e}\right) m_2 g \tag{6.5}$$

These values are constant for our bicycle model on a flat road. For the road friction coefficient μ, a value of 0.8 is chosen. This is comparable to a truck tire on asphalt. Figure 6.2 shows the cornering stiffness of the different tires as function of the longitudinal force for these given conditions and a value for n of 2.

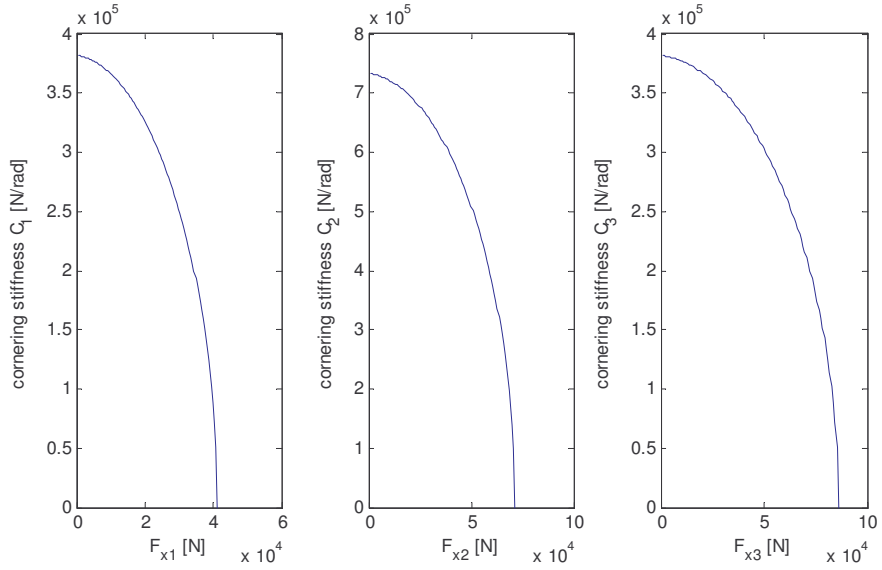

Figure 6.2 Cornering stiffness as function of longitudinal force

6.2 Stability

The stability of the system can be analyzed for different values of braking forces and brake force distributions. For this analysis, the eigenvalues can be evaluated as in section 5.1. A forward velocity of 20 m/s is chosen.

6.2.1 Braking on one axle

Table 6.1 shows the eigenvalues when the brake force is completely shifted to the front tire of the tractor.

Table 6.1 Eigenvalues for braking at the front tire of the tractor

F_{x1}=0 N, F_{x2}=F_{x3}=0 N				
Eigenvalue	**Value**	**ω_o [rad/s]**	**ω_n [rad/s]**	**ζ [-]**
λ_1	-0.0909	-	-	-
λ_2	-4.0683+1.3023i	4.2717	1.3023	0.9524
λ_3	-4.0683-1.3023i	4.2717	1.3023	0.9524
λ_4	-3.9993	-	-	-
F_{x1}=20000 N, F_{x2}=F_{x3}=0 N				
Eigenvalue	**Value**	**ω_o [rad/s]**	**ω_n [rad/s]**	**ζ [-]**
λ_1	-3.7805+2.0096i	4.2815	2.0096	0.8830
λ_2	-3.7805-2.0096i	4.2815	2.0096	0.8830
λ_3	-0.0909	-	-	-
λ_4	-4.0001	-	-	-
F_{x1}=40000 N, F_{x2}=F_{x3}=0 N				
Eigenvalue	**Value**	**ω_o [rad/s]**	**ω_n [rad/s]**	**ζ [-]**
λ_1	-2.5177+3.5180i	4.3261	3.5180	0.5820
λ_2	-2.5177-3.5180i	4.3261	3.5180	0.5820
λ_3	-0.0910	-	-	-
λ_4	-4.0006	-	-	-

From this table, it can be concluded that a larger brake input on the front tires of the tractor causes the system to be less stable. Especially at 40000 N brake input, which is close to front wheel lock (figure 6.2), the system becomes less stable. Although the system remains stable, the eigenvalues are closer to the imaginary axis and the damping drops to 58%.

Table 6.2 shows the eigenvalues when the brake force is completely shifted to the rear tire of the tractor.

Table 6.2 Eigenvalues for braking at the rear tire of the tractor

F_{x2}=0 N, F_{x1}=F_{x3}=0 N				
Eigenvalue	**Value**	**ω_o [rad/s]**	**ω_n [rad/s]**	**ζ [-]**
λ_1	-0.0909	-	-	-
λ_2	-4.0683+1.3023i	4.2717	1.3023	0.9524
λ_3	-4.0683-1.3023i	4.2717	1.3023	0.9524
λ_4	-3.9993	-	-	-
F_{x2}=35000 N, F_{x1}=F_{x3}=0 N				
Eigenvalue	**Value**	**ω_o [rad/s]**	**ω_n [rad/s]**	**ζ [-]**
λ_1	-0.0909	-	-	-
λ_2	-2.7691	-	-	-
λ_3	-4.8424	-	-	-

λ_4	-3.9045	-	-	-
F_{x2}=70000 N, F_{x1}=F_{x3}=0 N				
Eigenvalue	**Value**	**ω_o [rad/s]**	**ω_n [rad/s]**	**ζ [-]**
λ_1	-6.3800	-	-	-
λ_2	1.6488	-	-	-
λ_3	-0.0911	-	-	-
λ_4	-3.9586	-	-	-

At 70000 N brake input, which is close to tractor rear wheel lock, one of the eigenvalues becomes positive. This means that the vehicle becomes unstable. Clearly, this braking option is not desirable.

Table 6.3 shows the eigenvalues when the brake force is completely shifted to the trailer tire.

Table 6.3 Eigenvalues for braking at the trailer tire

F_{x3}=0 N, F_{x1}=F_{x2}=0 N				
Eigenvalue	**Value**	**ω_o [rad/s]**	**ω_n [rad/s]**	**ζ [-]**
λ_1	-0.0909	-	-	-
λ_2	-4.0683+1.3023i	4.2717	1.3023	0.9524
λ_3	-4.0683-1.3023i	4.2717	1.3023	0.9524
λ_4	-3.9993	-	-	-
F_{x3}=43000 N, F_{x1}=F_{x2}=0 N				
Eigenvalue	**Value**	**ω_o [rad/s]**	**ω_n [rad/s]**	**ζ [-]**
λ_1	-4.0940+1.3170i	4.3006	1.3170	0.9520
λ_2	-4.0940-1.3170i	4.3006	1.3170	0.9520
λ_3	-0.0913	-	-	-
λ_4	-3.3336	-	-	-
F_{x3}=86000 N, F_{x1}=F_{x2}=0 N				
Eigenvalue	**Value**	**ω_o [rad/s]**	**ω_n [rad/s]**	**ζ [-]**
λ_1	-4.0882+1.3646i	4.3100	1.3646	0.9486
λ_2	-4.0882-1.3646	4.3100	1.3646	0.9486
λ_3	-0.0933+0.0887i	0.1288	0.0887	0.7246
λ_4	-0.0933-0.0887i	0.1288	0.0887	0.7246

From this table, it can be seen that a brake force of 43000 N does not give a big change in stability of the vehicle. However, at 86000 N (close to trailer wheel lock) another pair of complex conjugated eigenvalues exists. This pair has a much lower eigenfrequency and damping ratio of 72%. Although the system remains stable, a simulation at trailer wheel lock shows that two of the eigenvalues have a real part that is exactly equal to 0 and the damping ratio drops to 0%.

6.2.2 Braking on tractor tires

There are two options when the brake force is chosen to be on the tractor tires only. One can choose for an equal brake force distribution and a brake force distribution causing equal slip at the tires. This is shown in tables 6.4 and 6.5.

Table 6.4 Eigenvalues for braking at the tractor (equal brake forces)

F_{x1}=F_{x2}=0 N, F_{x3}=0 N				
Eigenvalue	**Value**	**ω_o [rad/s]**	**ω_n [rad/s]**	**ζ [-]**
λ_1	-0.0909	-	-	-
λ_2	-4.0683+1.3023i	4.2717	1.3023	0.9524
λ_3	-4.0683-1.3023i	4.2717	1.3023	0.9524
λ_4	-3.9993	-	-	-
F_{x1}=F_{x2}=20000 N, F_{x3}=0 N				
Eigenvalue	**Value**	**ω_o [rad/s]**	**ω_n [rad/s]**	**ζ [-]**
λ_1	-3.6660+1.7751i	4.0732	1.7751	0.9000
λ_2	-3.6660-1.7751i	4.0732	1.7751	0.9000
λ_3	-0.0909	-	-	-
λ_4	-4.0095	-	-	-
F_{x1}=F_{x2}=40000 N, F_{x3}=0 N				
Eigenvalue	**Value**	**ω_o [rad/s]**	**ω_n [rad/s]**	**ζ [-]**
λ_1	-2.1119+3.1615i	3.8020	3.1615	0.5555
λ_2	-2.1119-3.1615i	3.8020	3.1615	0.5555
λ_3	-0.0910	-	-	-
λ_4	-4.0030	-	-	-

Table 6.5 Eigenvalues for braking at the tractor (equal slip)

F_{x1}=0 N, F_{x2}=0 N, F_{x3}=0 N				
Eigenvalue	**Value**	**ω_o [rad/s]**	**ω_n [rad/s]**	**ζ [-]**
λ_1	-0.0909	-	-	-
λ_2	-4.0683+1.3023i	4.2717	1.3023	0.9524
λ_3	-4.0683-1.3023i	4.2717	1.3023	0.9524
λ_4	-3.9993	-	-	-
F_{x1}=20000 N, F_{x2}=35000 N, F_{x3}=0 N				
Eigenvalue	**Value**	**ω_o [rad/s]**	**ω_n [rad/s]**	**ζ [-]**
λ_1	-3.4465+1.2202i	3.6561	1.2202	0.9427
λ_2	-3.4465+1.2202i	3.6561	1.2202	0.9427
λ_3	-4.0483	-	-	-
λ_4	-0.0909	-	-	-
F_{x1}=40000 N, F_{x2}=70000 N, F_{x3}=0 N				
Eigenvalue	**Value**	**ω_o [rad/s]**	**ω_n [rad/s]**	**ζ [-]**
λ_1	-4.0141	-	-	-
λ_2	-0.0899	-	-	-
λ_3	-0.6806	-	-	-
λ_4	-0.8964	-	-	-

From tables 6.4 and 6.5, it can be concluded that an equal brake force distribution causes the system to be more stable than a brake force distribution with equal slip. This is because the real parts of the eigenvalues of the equal brake force distribution are further away from a value of 0. However, the front tire of the tractor locks up first in this configuration and the steering response of the vehicle is much worse.

6.2.3 Braking on all tires

As in section 6.2.2, one can choose for an equal brake force distribution or a brake force distribution causing equal slip at the tires. This is shown in tables 6.6 and 6.7.

Table 6.6 Eigenvalues for braking on all tires (equal brake forces)

$F_{x1}=F_{x2}=F_{x3}=0$ N				
Eigenvalue	**Value**	**ω_o [rad/s]**	**ω_n [rad/s]**	**ζ [-]**
λ_1	-0.0909	-	-	-
λ_2	-4.0683+1.3023i	4.2717	1.3023	0.9524
λ_3	-4.0683-1.3023i	4.2717	1.3023	0.9524
λ_4	-3.9993	-	-	-
$F_{x1}=F_{x2}=F_{x3}=20000$ N				
Eigenvalue	**Value**	**ω_o [rad/s]**	**ω_n [rad/s]**	**ζ [-]**
λ_1	-3.6702+1.7743i	4.0766	1.7743	0.9003
λ_2	-3.6702-1.7743i	4.0766	1.7743	0.9003
λ_3	-0.0910	-	-	-
λ_4	-3.8497	-	-	-
$F_{x1}=F_{x2}=F_{x3}=40000$ N				
Eigenvalue	**Value**	**ω_o [rad/s]**	**ω_n [rad/s]**	**ζ [-]**
λ_1	-2.1152+3.1599i	3.8025	3.1599	0.5563
λ_2	-2.1152-3.1599i	3.8025	3.1599	0.5563
λ_3	-0.0913	-	-	-
λ_4	-3.4629	-	-	-

Table 6.7 Eigenvalues for braking on all tires (equal slip)

$F_{x1}=0$ N, $F_{x2}=0$ N, $F_{x3}=0$ N				
Eigenvalue	**Value**	**ω_o [rad/s]**	**ω_n [rad/s]**	**ζ [-]**
λ_1	-0.0909	-	-	-
λ_2	-4.0683+1.3023i	4.2717	1.3023	0.9524
λ_3	-4.0683-1.3023i	4.2717	1.3023	0.9524
λ_4	-3.9993	-	-	-
$F_{x1}=20000$ N, $F_{x2}=35000$ N, $F_{x3}=42500$ N				
Eigenvalue	**Value**	**ω_o [rad/s]**	**ω_n [rad/s]**	**ζ [-]**
λ_1	-0.0913	-	-	-
λ_2	-3.4743+1.2095i	3.6788	1.2095	0.9444
λ_3	-3.4743-1.2095i	3.6788	1.2095	0.9444
λ_4	-3.3923	-	-	-

F_{x1}=40000 N, F_{x2}=70000 N, F_{x3}=85000 N				
Eigenvalue	**Value**	**ω_o [rad/s]**	**ω_n [rad/s]**	**ζ [-]**
λ_1	-0.1074	-	-	-
λ_2	-1.0033	-	-	-
λ_3	-0.4621	-	-	-
λ_4	-0.6736	-	-	-

From tables 6.6 and 6.7, it can be concluded that an equal brake force distribution causes the system to be more stable than a brake force distribution with equal slip. This is because the real parts of the eigenvalues of the equal brake force distribution are further away from a value of 0. However, the front tire of the tractor locks up first in this configuration and the steering response of the vehicle is much worse.

6.3 Conclusions

Cornering stiffness is a system parameter that is dependent on variables such as vertical load on the tire, road friction coefficient and braking force. In this chapter, it is investigated how different ways of braking influences the cornering stiffness and thus the stability of the system. Although the brake force is not directly included in the equations of motions, this gives a good indication how different braking strategies influence the stability of the system. Braking on the front tires of the tractor cannot cause the system to become unstable unlike braking on the rear tires of the tractor. Although braking on the trailer tires cannot cause the system to become unstable, it makes the system less stable and can cause the trailer to ‘swing’. Although shifting the brake force towards the front tires of the tractor seems the best option, it causes the steering response to become much worse during braking. A compromise has to be made between the ability to brake and the ability to steer.

7. Active Yaw Control

7.1 Working principle

An Active Yaw Control (AYC) system is an augmentation to a Anti-lock Braking System (ABS). The main objective of an AYC system is to maintain a small vehicle side slip angle under all driving conditions. This is achieved through proper control of the vehicle yaw moment. There are two major types of AYC designs: the phase plane approach and the simultaneous yaw rate/vehicle side slip control designs. The phase plane approach utilizes the phase plane analysis to characterize the vehicle lateral stability. The control action is activated when the vehicle states enter the unstable regions. This approach requires identifying the boundaries of the stable and unstable region under different steering angles and vehicle speed. The latter approach requires estimations of the desired yaw rate and side slip angle based on driver's inputs and vehicle states.

The evaluation problem of an AYC system can be regarded as a two-player worst-case evaluation (section 3.1). The control player (the AYC controller) tries to maintain yaw stability, while the disturbance player, which controls the steering and brake pressure, represents the action of a human driver.

The worst-case AYC evaluation problem is stated below [5]:

Given a nonlinear vehicle dynamic model $\dot{\underline{x}} = f(\underline{x}, \underline{u}, \underline{w}, t)$, *where the disturbance input* $\underline{w}$ *includes front wheel steering angle* δ *and brake pedal command* p. *The control input* $\underline{u}$ *includes the ABS pressure command* p_{ABS} *and AYC pressure command* p_{AYC}. *The final brake pressure to the vehicle wheels depends on the three pressure command signals. Assuming that the control algorithms of the ABS and AYC modules are known. Find, within saturation bound* $-\delta_{\max} \le \delta \le \delta_{\max}$ *and* $0 \le p \le p_{\max}$, *the time signal* $\underline{w}(t)$ *which maximizes a cost function* $J(\underline{x}, \underline{w}, t) = \int_0^T \left\{ \underline{x}^T(t) Q \underline{x}(t) + \underline{u}^T(t) R \underline{u}(t) - \underline{w}^T(t) P \underline{w}(t) \right\} dt$. *The matrix* Q *is selected such that the vehicle side slip angle is maximized.*

Two assumptions are made concerning AYC systems:

- AYC only increases the brake pressure on one of the front wheels. It never reduces brake pressure.
- The overall brake pressure applied to the tires is the sum of the three brake command signals from the ABS (P_{ABS}), AYC (P_{AYC}), and the driver (P_{drv}). This is illustrated in figure 7.1.

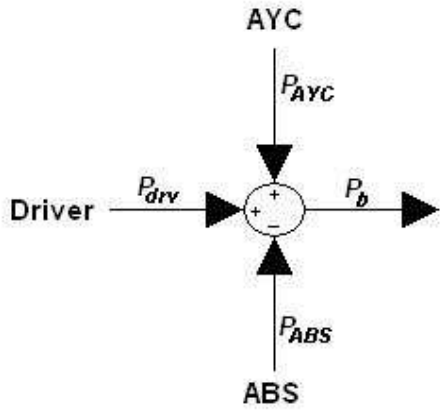

Figure 7.1 The Brake Model

7.2 Simulation

Simulations have been done where a standard passenger vehicle model is augmented with an AYC control system [5]. The AYC design used here is a yaw-rate feedback approach. When the vehicle side slip angle is greater than a threshold, AYC is activated. The magnitude of AYC braking is calculate from

$$\Delta P_{AYC} = C_{AYC1}\left|r - r_d\right| + C_{AYC2}\left|\beta + C_{AYC3}\dot{\beta}\right| \tag{7.1}$$

with:

$C_{AYC1}, C_{AYC2}, C_{AYC3}$ = control gains

r_d = desired yaw rate

β = vehicle side slip angle

The differential braking from AYC is applied only to the front tires. When β is positive and larger than a threshold, the AYC activates the front right tire. Similarly, if β is negative and less than a threshold, the brake pressure at the front left is increased.

The effectiveness of the AYC is first examined under three standard maneuvers: brake in a J-turn, double lane changes and the worst-case maneuver. Simulation results under a double lane change maneuver are shown in figure 7.2. It can be seen that the vehicle without AYC lost control when the steering direction is reversed. The vehicle with AYC, however, remains stable.

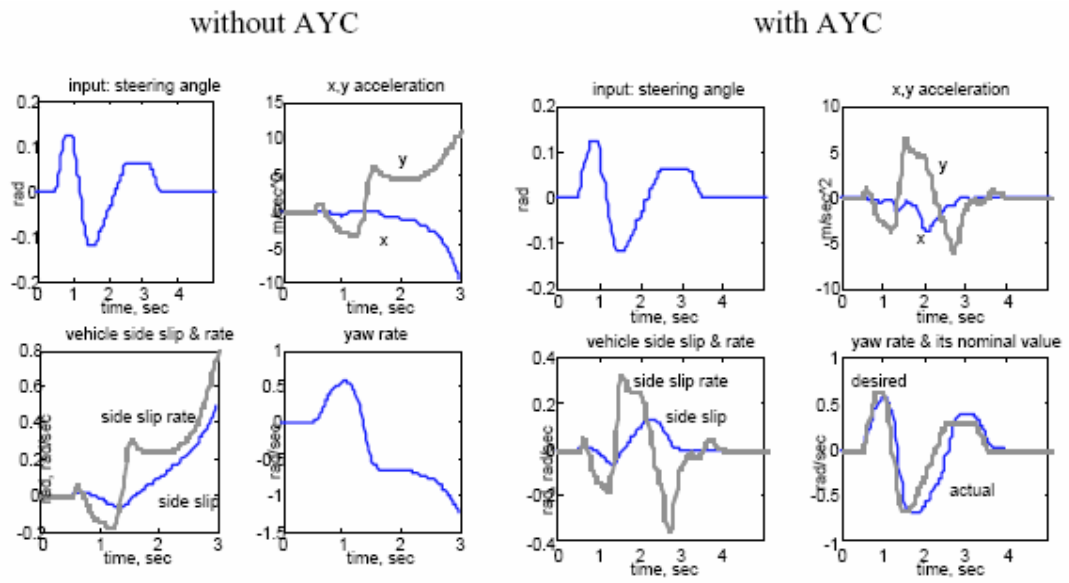

Figure 7.2 Vehicle response under a double lane-change maneuver, source: [5]

Figure 7.3 shows the vehicle, equipped with AYC, under two different maneuvers. Under the brake in a J-turn maneuver, the steering and braking input limits are 0.05 rad and 300 psi, respectively. The vehicle remains stable under this severe maneuver.

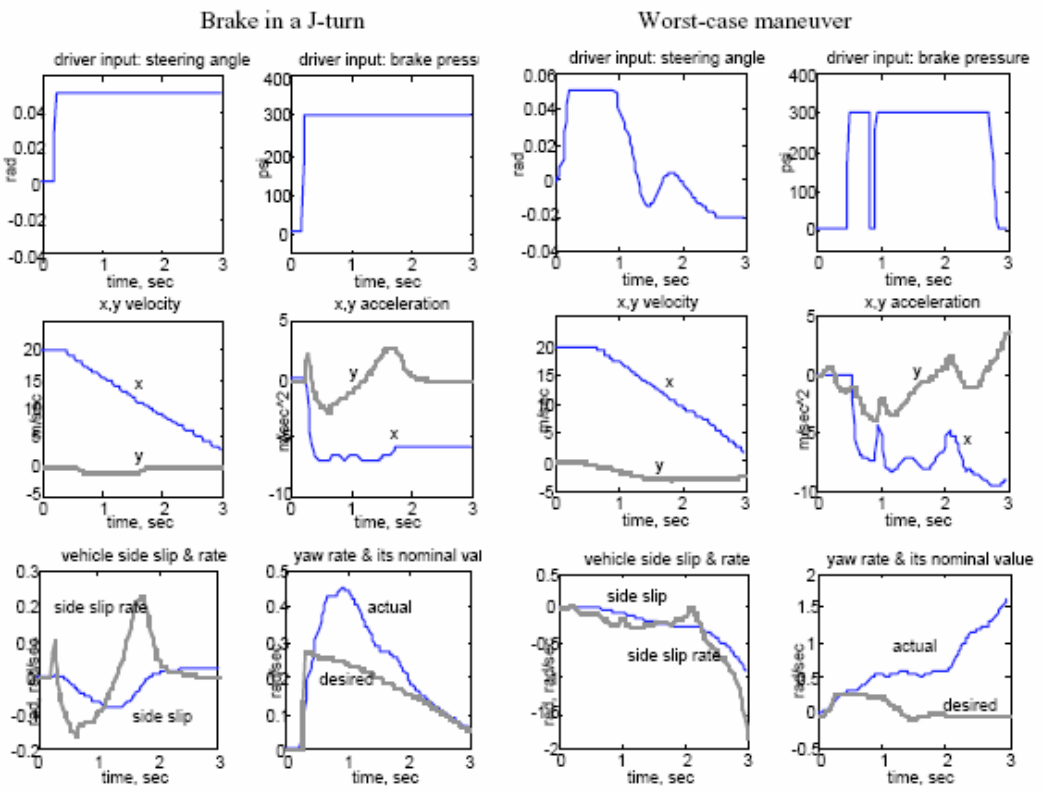

Figure 7.3 Response of an AYC vehicle under two maneuvers, source: [5]

7.3 Conclusions

AYC systems use adjustable brake forces on separate wheels to maintain a small vehicle side slip angle. Although an AYC control system has proven itself already in experiments for passenger cars, it has not been implemented in tractor-semitrailer combinations yet. Because of the extra variables concerning the tractor-semitrailer combination with respect to a passenger car, designing a control law for such a combination is much harder and therefore has not been implemented yet in articulated vehicles.

8. Active Front Steering

8.1 Working principle

Active Front Steering (AFS) is a new advanced steering system. The handwheel angle in this system is augmented by an electronically controlled electric motor.

Because of the development of hybrid electric-diesel trucks with electric driven accessories, it becomes interesting to investigate AFS for large trucks to assist in avoiding jackknife conditions. In order to effectively deploy this technology in commercial fleet operations, emphasis is given to design aspects to minimize the tendency of AFS systems to interfere with the driver's perception of the truck dynamic response.

Drive-by-wire systems have been under development for a number of years for the passenger vehicle market. In these systems, the chassis has a mechanism to provide an additive steering angle component to the driver's input. This augmented steering input can be used to modify the effective steering gear ratio. With electronic control, the gear ratio is continuously varied. Depending upon speeds the ratio is increased. However, during rapid acceleration and deceleration, AFS may cause enough variation to confuse the driver about how the steering system is responding. This situation can occur in emergency conditions for example. For these types of conditions, additional development is needed to incorporate yaw rate and lateral acceleration sensors into the control of the AFS system.

Electronically controlled steering for large commercial vehicles is motivated by improving public safety. The AFS system improves the stability of the tractor-trailer, but may modify the dynamic response to a point where the driver begins to perceive a disconnection between steering handwheel inputs and the resulting behavior of the vehicle.

An AFS mechanism as described in [9] is shown in figure 8.1.

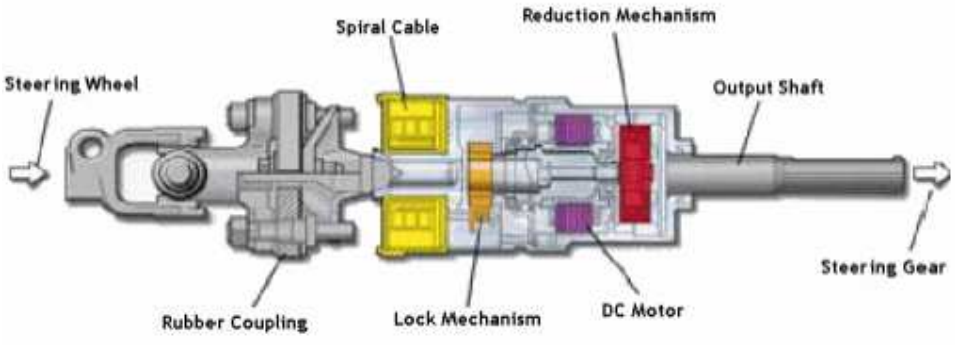

Figure 8.1 AFS mechanism, source: [10]

The AFS assembly consists of two planetary gear sets with a torque input from the handwheel and a separate torque input path from an electric servo motor. These two

torque inputs are summed together at the output shaft. The dual planetary mechanism allows for position isolation between the two torque inputs. In this manner, the actual steering angle of the front axle wheels can be adjusted independently of the driver's input. The AFS augmenting steering angle is limited to a maximum deflection to prevent a completely uncontrollable situation arising due to a fault condition. However, small angle displacements are significant at highway speeds and therefore AFS is a safety critical system. The AFS system is fail-safe, since a loss of power to the electric servo motor results in a normal mechanical steering operation.

The controller in an AFS system uses the measured signals handwheel position, longitudinal velocity, yaw rate and lateral velocity for both the tractor and trailer, and brake apply status. An electronic controller receives the sensor inputs and processes the data to determine an augmentation steering angle. This angle is then executed through a servo motor as a component of the AFS system. A block diagram of this configuration is shown in figure 8.2.

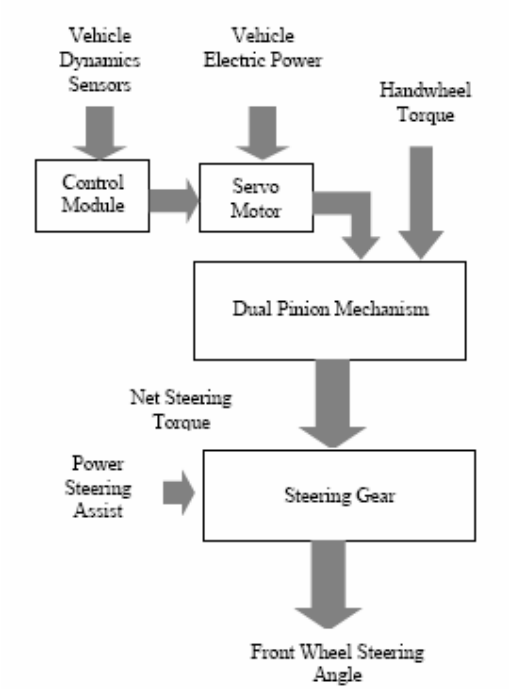

Figure 8.2 AFS configuration, source: [10]

The dynamics associated with the application of a torque to the steering mechanism to the resulting steering angle are

$$J_s\ddot{\delta} = -B_s\dot{\delta} - K_s\alpha_1 + \tau_{hw} - \tau_{afs} \tag{8.1}$$

with:

J_s = inertia of the steering system

δ = steering angle

B_s = damping of the steering system

K_s = self-aligning stiffness of the tires

α_1 = side slip angle of the front tires

τ_{hw} = handwheel torque

τ_{afs} = AFS torque

In most cases, a jackknife or rollover event is caused by traveling at higher speeds that can be negotiated by the tractor-trailer. It is intended that AFS would be incorporated as part of an enhanced stability system that includes electronically controlled brakes.

The formulation of the control law for the AFS torque is complicated by the large variation and uncertainty in the conditions under which the tractor-trailer may be operated. The design of stability enhancement systems often is based upon gain scheduling of feedback control laws to account for vehicle dynamic changes as a function of vehicle speed. Although this gives a technically optimal control, this can cause the driver to perceive that the vehicle behavior is unpredictable. This tends to increase the problem of controlling the vehicle under emergency conditions. Thus, the control for AFS using constant state feedback of the vehicle dynamics variables is preferred. The form of the AFS control law is given as

$$\tau_{afs} = k_1 v_1 + k_2 r_1 + k_3 r_2 + k_4 \gamma + k_5 \dot{v}_1 \tag{8.2}$$

with:

k_i = AFS control gains

v_1 = tractor lateral velocity

r_1 = tractor yaw rate

r_2 = trailer yaw rate

γ = articulation angle

8.2 Simulation

Simulations have been done with an AFS system. The particular situation examined is a rapid braking and lane change of a large truck at 70 mph. This happens for example when avoiding a rear-end collision with a stopped or rapidly decelerating passenger car on an interstate highway. The truck simultaneously brakes to decelerate in the longitudinal direction and steers to the center of the left lane in order to avoid colliding with the preceding passenger car.

The dynamics of human operator as part of a closed-loop system is an extensive area of study for which there is a considerable body of literature. This study is further complicated by the large number of variables that affect the performance of a human driver. This includes experience level and familiarity with the particular tractor-trailer. Road conditions and visibility are also important variables. In addition, the fatigue

level and alertness of the driver are critical factors. This research considers a simplified human model that captures the primary dynamics of interest without unnecessarily complicating the overall model.

The scenario is selected such that a driver of average skill would not be able to avoid a collision with jackknifing the vehicle. AFS position control is limited to +/- 4.5 degrees (tire coordinates). At highway speeds, tire angle changes of 0.5 degrees are perceptible to the driver. The AFS angle is additive (plus or minus) to the handwheel angle. The articulation angle with and without AFS is shown for a simulated condition in figure 8.3.

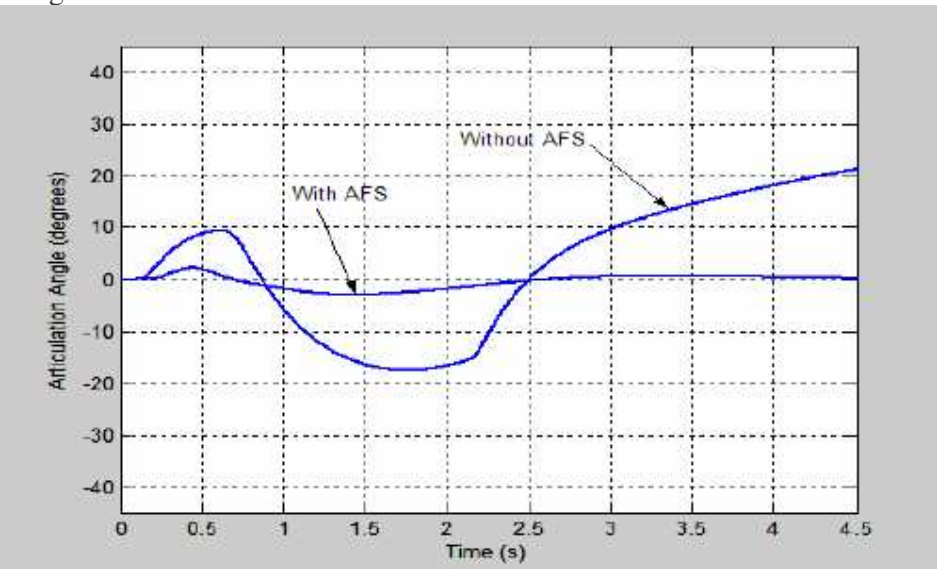

Figure 8.3 Articulation angle comparison for simulated evasive maneuver, source: [10]

In general, as the AFS level is decreased, the tractor-trailer becomes less stable and has correspondingly large path and angle instabilities. As the AFS torque level is increased, the tractor-trailer is stabilized, but at the expense of potentially creating an interference situation with the driver performance. The lane position results for various AFS factors are shown in figure 8.4.

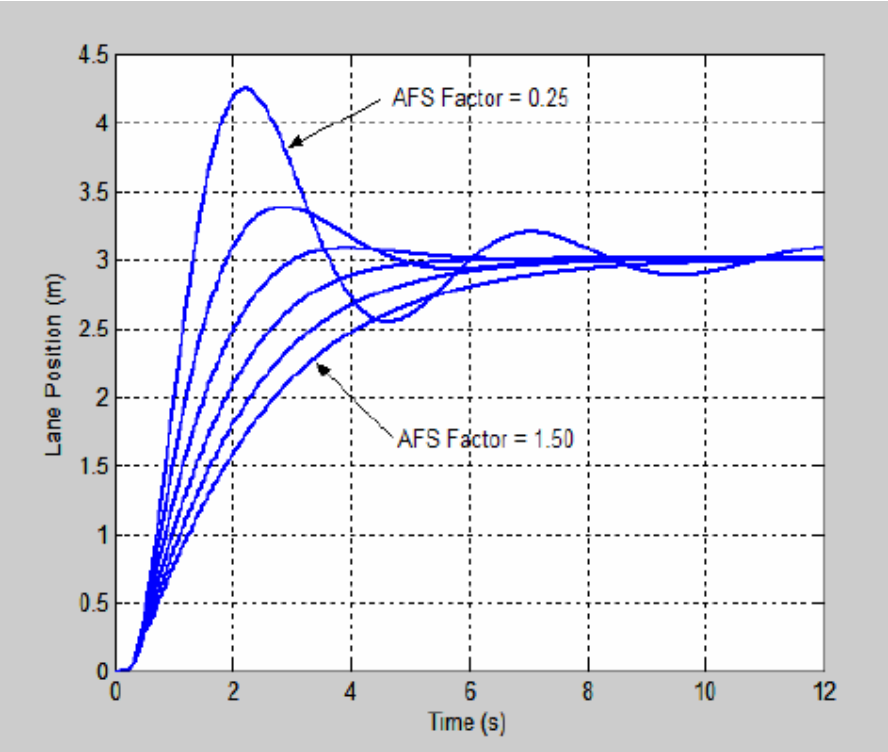

Figure 8.4 Lane position for various AFS factors, source: [10]

8.3 Conclusions

An AFS system uses an electronically controlled electric motor to augment the handwheel steering angle to maintain stability. The AFS system improves the stability of the tractor-trailer, but may modify the dynamic response to a point where the driver begins to perceive a disconnection between steering handwheel inputs and the resulting behavior of the vehicle. This has to be avoided, because it can result in unpredictable steering behavior of the driver. Simulations show that AFS can improve stability of articulated vehicles when adjusted properly.

9. Conclusions and recommendations

In this report, the jackknife stability of a tractor semi-trailer combination is examined. In order to do so, a linear bicycle model is build for the combination. After that, a way to determine the worst possible steering and braking inputs is analyzed, but is not used in the simulations that are done with the model. This is because the stability of a linear bicycle model does not change during different maneuvers. However, the worst-case evaluation can be used for simulations of a 3D model. To determine what causes jackknife instability, an analysis is done for a simplified linear bicycle model. This analysis includes linear simulations with Matlab and an analysis of the eigenvalues of the system for various values of different vehicle parameters. Although braking forces are not directly included in the equations of motion of the vehicle, an analysis is done on the effects of braking forces on the cornering stiffness of tires. This analysis is done because the cornering stiffness of tires, unlike other system parameters in the linear bicycle model, is not constant, but varies during different maneuvers. With the effect of braking force on cornering stiffness being known, an analysis of the eigenvalues of the system is done for various braking possibilities. Finally, two systems that can prevent jackknife instability are discussed. An Active Yaw Control system uses variable braking forces on separate tires, whereas an Active Front Steering system uses a variable steering gear ratio.

To determine the jackknife stability of a tractor semi-trailer combination, a linear bicycle model is used in this report. Although this is a possibility to determine certain trends that can cause instability, this is not a way to determine stability for an existing truck. This is because the linear bicycle model does not include some effects that are present in a 3D space. A few of these effects are:

- Load transfer on the tires between the left and right side of the vehicle during cornering. This affects the cornering stiffness of tires and the deflection of the suspension which causes roll motions.
- Load transfer on the tires between the front and rear side of the vehicle during braking. This affects the cornering stiffness of tires and the deflection of the suspension which causes pitch motions.
- Displacement of the centers of gravity of the tractor and trailer due to pitch and roll motions.

In order to determine the stability of existing trucks, a 3D model needs to be used to take these effects into account. Furthermore, the system parameters are assumed to be constant. When the system parameters are not assumed to be constant, the analysis of eigenvalues is not a valid way to determine the stability of the system. In this case, an other way such as Lyapunov stability analysis can be used.

References

[1] Starnes, M., “Large-Truck Crash Causation Study: An Initial Overview”, NHTSA Technical Report, Springfield, Viginia, August 2006.

[2] Runge, J.W., “Traffic Safety Facts 2003: A Compilation of Motor Vehicle Crash Data from the Fatality Analysis Reporting System and the General Estimates System”, NHTSA Technical Report, Washington, DC, January 2005.

[3] Pacejka, H. B., “Tyre and Vehicle Dynamics”, Elsevier, Oxford, United Kingdom, 2004.

[4] Ma, W. and Peng, H., “Worst-case Maneuvers for the Roll-over and Jackknife of Articulated Vehicles”, *Proceedings of the American Control Conference*, Philadelphia, Pennsylvania, 1998.

[5] Ma, W. and Peng, H., “Worst-case Vehicle Evaluation Methodology – Examples on Truck Rollover/Jackknifing and Active Yaw Control Systems”, *Vehicle System Dynamics*, Vol. 32, p. 389-408, 1999.

[6] Bryson, A. E., and Ho, Y.C., “Applied Optimal Control; Optimization, Estimation, and Control”, Blaisdell Pub. Co., London, 1969.

[7] Dugoff, H., Ervin, R. D., and Segel, L., “Vehicle Handling Test Procedures”, Transportation Research Institute, University of Michigan, Report Contract No. FH-11-7297, 1970.

[8] Dunn, A. L., “Jackknife Stability of Articulated Tractor Semitrailer Vehicles with High-Output Brakes and Jackknife Detection on Low Coefficient Surfaces”, Ohio State University, Columbus, Ohio, 2003.

[9] West, T. “BMW’s New Steering System Leaves Us Wanting Less”, *Popular Science*, October 2003.

[10] McCann, R. and Le A., “Electric Motor Based Steering for Jackknife Avoidance in Large Trucks”, *IEEE Vehicle Power and Propulsion*, Issue 7-9 September, 2005.

Appendix A

$$M = \begin{bmatrix} m_1 + m_2 & -(c+d)m_2 & -dm_2 & 0 \\ -(c+d)m_2 & J_1 + J_2 + (c+d)^2 m_2 & J_2 + d(c+d)m_2 & 0 \\ -dm_2 & J_2 + d(c+d)m_2 & J_2 + d^2 m_2 & 0 \\ 0 & 0 & 0 & 1 \end{bmatrix}$$

$$K = \frac{1}{u}\begin{bmatrix} -(C_1 + C_2 + C_3) & -aC_1 + bC_2 + (c+d+e)C_3 - (m_1 + m_2)u^2 \\ -aC_1 + bC_2 + (c+d+e)C_3 & -a^2 C_1 - b^2 C_2 - (c+d+e)^2 C_3 + (c+d)u^2 m_2 \\ (d+e)C_3 & -(d+e)(c+d+e)C_3 + dm_2 u^2 \\ 0 & 0 \end{bmatrix}$$

$$\begin{bmatrix} (d+e)C_3 & uC_3 \\ -(d+e)(c+d+e)C_3 & -(c+d+e)uC_3 \\ -(d+e)^2 C_3 & -(d+e)uC_3 \\ 1 & 0 \end{bmatrix}$$

$$B_1 = \begin{bmatrix} C_1 \\ aC_1 \\ 0 \\ 0 \end{bmatrix}$$